Elsevier Editorial System(tm) for Water Research or its open access mirror
Manuscript Draft

Manuscript Number: WR51163R2

Title: Impact of Salt Accumulation in the Bioreactor on the Performance of Nanofiltration Membrane Bioreactor (NF-MBR)+Reverse Osmosis (RO) Process for Water Reclamation

Article Type: Research Paper

Keywords: Membrane bioreactor; Membrane fouling; Nanofiltration; Reverse Osmosis; Salt accumulation; Water reclamation

Corresponding Author: Dr. Tzyy Haur Chong, PhD

Corresponding Author's Institution: Nanyang Technological University

First Author: Ming Feng Tay

Order of Authors: Ming Feng Tay; Seonki Lee; Huijuan Xu; Kwanho Jeong; Chang Liu; Emile Cornelissen; Bing Wu; Tzyy Haur Chong, PhD

Abstract: The impacts of salt accumulation, through adjusting the solid retention time (SRT), in the bioreactor on the bioprocess as well as membrane performance of a high retention nanofiltration membrane bioreactor (NF-MBR) and subsequent reverse osmosis (RO) process for water reclamation are addressed in this study. The build-up of salts (i.e., Ca, Mg, PO4) is a function of SRT, hydraulic retention time (HRT) and membrane rejection. Despite the accumulation of salts, both NF-MBRs at SRT of 30 and 60 d, achieved (i) similar biodegradation efficiency; (ii) excellent organic removal (>97%); and (iii) ammonia removal (>98%). Extending the SRT could improve the microbial bio-flocculation capability, but did not influence the microbial activity, viability, and community structure. However, more severe membrane fouling was observed in the NF-MBR with elevated salt levels, which was attributed to the greater formation of calcium phosphate scale and Ca-polysaccharides complex (i.e., irreversible fouling layer) as well as the cake-enhanced-osmotic-pressure (CEOP) effect. Although both NF-MBRs produced comparable quality of permeate, a higher RO membrane fouling rate was observed when permeate of NF-MBR with SRT at 60 d was fed to the RO system, implying organic compositions in NF-MBR permeate may influence RO performance.

Highlights:

- Salt accumulation in the NF-MBR had no adverse impact on the bioprocess.
- The elevated divalent ions level promoted bio-flocculation.
- Longer SRT caused severe Ca-polysaccharides combined fouling in NF-MBR.
- Integration of NF-MBR with RO process for high recovery water reclamation.

Graphical Abstract:

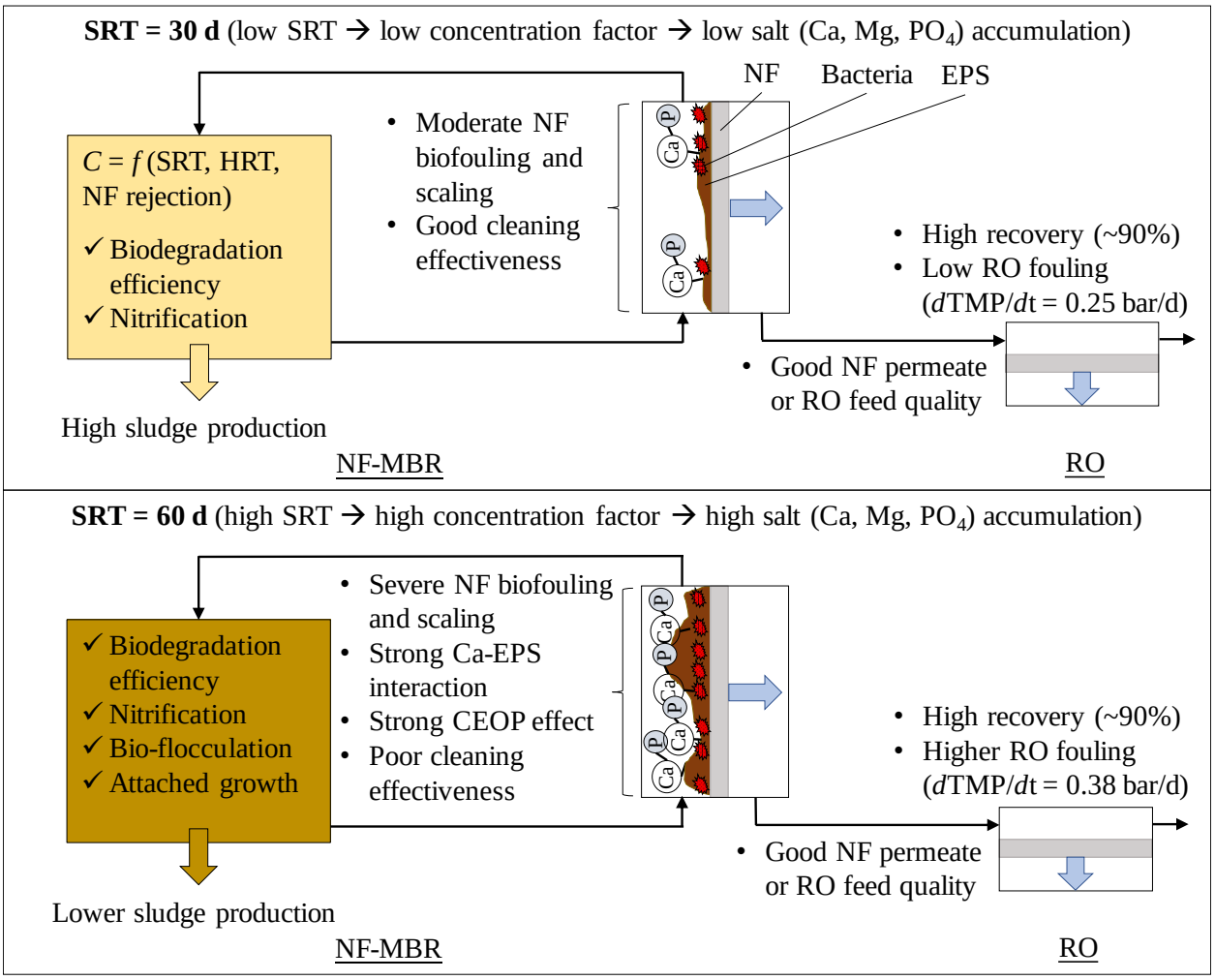

Impact of Salt Accumulation in the Bioreactor on the Performance of Nanofiltration Membrane Bioreactor (NF-MBR)+Reverse Osmosis (RO) Process for Water Reclamation

Ming Feng Tay [a,b], Seonki Lee[b], Huijuan Xu[b], Kwanho Jeong[b], Chang Liu [b, c]
Emile R. Cornelissen[b,d,e], Bing Wu [b,f]*, Tzyy Haur Chong [a,b]*

[a] School of Civil and Environmental Engineering, Nanyang Technological University, Singapore 639798, Singapore

[b] Singapore Membrane Technology Centre, Nanyang Environment and Water Research Institute, Nanyang Technological University, Singapore 637141, Singapore

[c] School of Environment and Resource, Southwest University of Science and Technology, 621010 Mianyang, China

[d] KWR Watercycle Research Institute, 3433 PE Nieuwegein, Netherlands

[e] Particle and Interfacial Technology Group, Ghent University, Coupure Links 653, B-9000 Ghent, Belgium

[f] Faculty of Civil and Environmental Engineering, University of Iceland, Hjardarhagi 2-6, IS-107 Reykjavik, Iceland

* Corresponding authors:

Tzyy Haur Chong, Email: thchong@ntu.edu.sg, Tel: +65 6513 8126, Fax: +65 6791 0676

Bing Wu, Email: wubing@hi.is

Abstract

The impacts of salt accumulation, through adjusting the solid retention time (SRT), in the bioreactor on the bioprocess as well as membrane performance of a high retention nanofiltration membrane bioreactor (NF-MBR) and subsequent reverse osmosis (RO) process for water reclamation are addressed in this study. The build-up of salts (i.e., Ca, Mg, PO_4) is a function of SRT, hydraulic retention time (HRT) and membrane rejection. Despite the accumulation of salts, both NF-MBRs at SRT of 30 and 60 d, achieved (i) similar biodegradation efficiency; (ii) excellent organic removal (>97%); and (iii) ammonia removal (>98%). Extending the SRT could improve the microbial bio-flocculation capability, but did not influence the microbial activity, viability, and community structure. However, more severe membrane fouling was observed in the NF-MBR with elevated salt levels, which was attributed to the greater formation of calcium phosphate scale and Ca-polysaccharides complex (i.e., irreversible fouling layer) as well as the cake-enhanced-osmotic-pressure (CEOP) effect. Although both NF-MBRs produced comparable quality of permeate, a higher RO membrane fouling rate was observed when permeate of NF-MBR with SRT at 60 d was fed to the RO system, implying organic compositions in NF-MBR permeate may influence RO performance.

Keywords: Membrane bioreactor; Membrane fouling; Nanofiltration; Reverse Osmosis; Salt accumulation; Water reclamation

Abbreviations

CEOP	Cake enhanced osmotic pressure
CF	Concentration factor
CLSM	Confocal laser scanning microscopy

COD	Chemical oxygen demand
tCOD	Total chemical oxygen demand
sCOD	Soluble chemical oxygen demand
DOC	Dissolved organic carbon
EPS	Extracellular polymeric substances
F/M	Food to microorganism ratio
HR-MBR	High retention membrane bioreactor
HRT	Hydraulic retention time
LC-OCD	Liquid chromatography – organic carbon detection
LMW	Low molecular weight
MBR	Membrane bioreactor
MLSS	Mixed liquor suspended solids
MLVSS	Mixed liquor volatile suspended solids
MWCO	Molecular weight cut-off
NF-MBR	Nanofiltration membrane bioreactor
SMP	Soluble microbial products
SOUR	Specific oxygen uptake rate
SRT	Solids retention time
TDS	Total dissolved solids
TOC	Total organic carbon

Symbols

C_f	Feed salt concentration
C_{ml}	Mixed liquor salt concentration
η_{NF}	Nanofiltration membrane rejection rate

1. Introduction

Recently, high retention membrane bioreactors (HR-MBRs), integrating a biological process with a high rejection membrane such as nanofiltration (NF), forward osmosis (FO), and membrane distillation (MD), have received significant attention in the field of wastewater reclamation due to their improved permeate quality as compared to conventional microfiltration (MF) or ultrafiltration (UF) based MBR (Lay et al. 2010, Luo et al. 2014). In MD-MBR, clean water can be achieved in a single step while additional step is required to recover the clean water from the draw solution in FO-MBR. Whereas in NF-MBR, with the improved MBR permeate as RO feed, the subsequent RO process can be potentially operated at higher recovery rate due to less RO fouling (Tay et al. 2018). In HR-MBRs, the high rejection membranes effectively retain the smaller size and refractory organic substances, leading to enhanced biodegradation (improved removal rates). However, the major disadvantage is the retention that leads to the accumulation of dissolved ions in the bioreactor by the high rejection membranes (Qiu and Ting 2013). It is noted that the concentration factor, CF, defined as the ratio of concentration of mixed liquor in the bioreactorto the feed concentration, is related to the sludge retention time (SRT) and hydraulic retention time (HRT), in which the maximum value, CF_{max} = SRT/HRT (Lay et al. 2010). Thus, SRT is an important parameter in determining salt accumulation ratio in HR-MBRs.

In conventional MF/UF-MBR, extending the SRT generally promoted lower soluble microbial products (SMP), lower specific bound EPS production, better bio-flocculation, and formation of a more permeable cake layer, therefore, resulting in less membrane fouling (Iorhemen et al. 2017, Massé et al. 2006, Ng et al. 2006, Van den Broeck et al. 2012, Wu et al. 2011). It is noted that longer SRT was often adopted to maintain high biomass concentrations (lower F/M ratio), reduce solids production, and minimize reactor volume (Pollice et al. 2004,

97 Xiao et al. 2019). In addition, longer SRT was preferred for more effective nitrification since the
98 autotrophic nitrifiers are very slow-growing microorganisms among other aerobic bacteria (Ge et
99 al. 2015).

100 On the other hand, in HR-MBRs, extending the SRT essentially means increasing the salt
101 accumulation, which can potentially impact the physical-chemical properties of the feed solution,
102 bioprocess, and membrane operation (Lay et al. 2010, Luo et al. 2014). For example, when
103 salinity increases, solubility of oxygen decreases linearly, which leads to lower oxygen transfer
104 rate (Colt 2012). This substantially reduces the effectiveness of aeration, which is translated into
105 higher energy requirement to achieve the desired DO level. Regarding the impact of salinity on
106 bioprocess, in both FO-MBR and MD-MBR, it has been found that elevated salinity could lead
107 to a shift in microbial community, lower growth yield and lower microbial kinetics of the
108 activated sludge necessary for the biological treatment and eventually resulted in process
109 deterioration (Luján-Facundo et al. 2018, Nawaz et al. 2013, Wijekoon et al. 2014). In term of
110 impact of salinity on membrane operation, in general, higher feed salinity means reduced net
111 driving force due to higher osmotic pressure difference and greater transport of solutes across the
112 membrane that lower the permeate flux and quality. In addition, accumulation of dissolved ions
113 such as Ca^{2+}, Mg^{2+}, SO_4^{2-}, PO_4^{3-}, etc. can increase the risk of membrane scaling and aggravate
114 colloidal fouling due to higher supersaturation index. Furthermore, the increase in extracellular
115 polymeric substances (EPS) production under high salinity environment as a protective
116 mechanism under salinity stress was found to increase the fouling propensity in FO-MBR (Qiu
117 and Ting 2013).

118 It shall be noted that most of the work reported on impacts of salt accumulation were
119 related to FO-MBR and MD-MBR, the in-depth study to address this issue for NF-MBR

application was not available. Indeed, research work on NF-MBR in the literature was rather limited, possibly associated with the poor permeability of NF membranes, typical flux was less than 5 L/m^{2}h (Choi et al. 2006, Choi et al. 2007, Phan et al. 2016, Zaviska et al. 2013), except in our previous work where flux of 10 L/m^{2}h was attained with the use of a low pressure in-house fabricated NF membrane (Tay et al. 2018). Therefore, it is unclear whether such observations found in FO-MBR and MD-MBR are applicable to NF-MBR. For instance, the driving force and membrane properties such as structure, permeability and rejection of FO, MD, and NF membranes differ from each other, which could have imposed different effects arisen from salt accumulation in the bioreactors on the bioprocess and membrane operation. Thus, in this study, the impacts of salt accumulation, through the manipulation of SRT, on microbial behaviors, bioreactor performance, permeate quality and membrane fouling of NF-MBR as well as the subsequent RO performance for water reclamation were investigated.

2. Materials and methods

2.1. NF-MBR setup and operating conditions

Two parallel lab-scale moving bed biofilm reactors employing side-stream NF membrane modules were used in this work. The schematic diagram of the NF-MBR is illustrated in Figure S1 (Appendix). The NF-MBRs were operated at SRT of 30 and 60 days (hereinafter denoted as NF-MBR_30-LS and NF-MBR_60-HS), respectively. Each bioreactor has a total effective working volume of 7.0 L and filled with 234 K3 bio-carriers (~20% of packing ratio). The dimension of bio-carrier is 12 mm × Ø 25 mm with surface area of 500 m^2/m^3 (Ping Yin Chemical Packing, China). The biofilm reactor was inoculated with aerobic activated sludge collected from a municipal wastewater treatment plant in Singapore at a mixed liquor suspended

solid (MLSS) concentration of 1 g/L. The aeration rate was set at 500 mL/min to maintain dissolved oxygen (DO) level above 4 mg/L. The hydraulic retention time (HRT), pH, and temperature were kept at 22 h, 6.8±0.5, and 20±0.5°C, respectively. The permeate flux of NF-MBR was maintained constant throughout the study at 10 L/m^{2}h via a mass flow controller installed on the permeate stream. The feed, retentate and permeate pressures were recorded by digital pressure transducers (Ashcroft, USA) connected to a data logging system (LabVIEW, National Instrument, USA). The municipal wastewater (after sieving with a 1 mm opening mesh) was collected weekly and stored in cool room at 4°C prior use as feed to NF-MBRs. The operating parameters of the NF-MBRs and the characteristics of the municipal wastewater are summarized in Tables 1 and 2, respectively.

Table 1. Operating parameters of NF-MBRs

Parameter	NF-MBR_30-LS	NF-MBR_60-HS
HRT (h)	22	22
SRT (d)	30	60
Flux (L/m^{2}h)	10	10
Organic loading rate (g Eq/L.day)	0.41	0.41
F/M ratio (g COD/g MLSS.d)	0.23	0.22
NF membrane crossflow velocity (m/s)	0.10	0.10
pH	6.2 – 6.9	6.2 – 6.9
Aeration (mL/min)	500	500
DO level (mg/L)	4.3-5.0	4.2-4.9
Biocarrier filling ratio (%)	20	20

Table 2. Characteristics of municipal wastewater (n=21)

Parameter	Level
tCOD (mg/L)	378.6 ± 116.5
sCOD(mg/L)	120.5 ± 28.3
DOC (mg/L)	55.3 ± 27.7
Ca^{2+} (mg/L)	26.1 ± 2.6
Mg^{2+} (mg/L)	10.4 ± 2.9
Na^{+} (mg/L)	99.0 ± 17.5
Fe^{3+} (mg/L)	0.45 ± 0.18
TN (mg/L)	39.7 ± 7.5

NH_4-N (mg/L)	39.3 ± 5.2
NO_3^--N (mg/L)	0.4 ± 0.1
NO_2^--N (mg/L)	N.D.
PO_4^{3-} (mg/L)	15.8 ± 2.6
TDS (mg/L)	666.4 ± 72.1
Conductivity (μs/cm)	970.7 ± 87.3

Note: tCOD: total chemical oxygen demand; sCOD: soluble chemical oxygen demand; DOC: dissolved organic carbon; TN: total nitrogen; N.D.: not detectable.

In this study, the in-house fabricated glutaraldehyde cross-linked layer-by-layer polyelectrolyte hollow fiber NF membranes with polyethersulfone (PES) UF as substrate were used and their characteristics are summarized in Table S1 (Appendix). The details of fabrication of this NF membrane can be found in the previous publication (Liu et al. 2015). Unlike most commercial NF membranes with high rejection (>90%) of divalent ions and partial rejection (i.e., 30 - 90%) of monovalent ions, this NF membrane does not reject monovalent ions while maintains high rejection of divalent ions, thus has low osmotic pressure difference across the membrane which allows low pressure operation, i.e., < 2 bar. Each membrane module consists of 40 (pieces of) hollow fibers (0.34 m in length with a total effective area of 0.031 m^2). The filtration was performed in an inside (lumen)-out (shell) configuration. Periodic physical cleaning (every two days) of membrane was performed in order to maintain constant permeate flux at 10 L/m^2h throughout the test. In detail, the fouled NF module was first removed from the NF-MBR and physical cleaning was conducted in a separate batch setup according to the following steps, i) flushing with tap water at 500 or 800 mL/min (equivalent to crossflow velocity of 0.5 or 0.8 m/s) for 30 s to remove clogged particles inside the lumen; ii) backwashing with ultrapure water at pressure of 2 or 3 bar for 15 min to detach the cake layer on the membrane surface; iii) flushing with tap water at 500 or 800 mL/min for 3 min to remove the residual foulants inside the lumen. After each physical cleaning cycle, the recovery of membrane permeability was checked by pure water flux measurement.

During first 30 days of operation, the mixed liquor in the bioreactor was directly fed to the NF membrane, denoted as NF1, which caused severe membrane fouling. Then, a sponge column (sponge pore size of ~ 0.5 mm, refer to Figure S1 in Appendix) was installed at the effluent outlet of the bioreactor before the NF module, aiming to retain the larger sized particles of >0.5 mm; a new NF membrane (NF2) was used in the subsequent test.

2.2. RO setup and operating conditions

Two identical RO systems were used to study the fouling potential of permeates from both NF-MBRs. The RO system consists of a feed tank, a high-pressure pump (Hydra Cell D-03-S, USA), a cooling device equipped with temperature controller (PolyScience 9106, USA), a flat sheet RO test cell, a back pressure regulator (SS-4R3A, Swagelok), a mass flow controller (LIQUI-FLOW L30, Bronkhorst, Netherlands), pressure transducers (EUTECH Instruments, USA), and conductivity meters (EUTECH Instruments, USA). The details of RO system were described previously (Suwarno et al. 2016, Tay et al. 2018, Wu et al. 2013). RO membrane (BW-30, DOW FilmTec, USA) with an effective membrane area of 0.0186 m^2 was employed in the RO test cell.

The RO membrane was first compacted with ultrapure water at flux of 50 L/m^2h and crossflow velocity of 0.10 m/s for 1 h prior fouling test. The RO feed water in the RO fouling test was the permeate collected from the NF-MBRs during Day 60-62. The collected NF-MBR permeate was first concentrated using the RO by discharging the RO permeate until its concentration equivalent to 90% recovery ratio, i.e., ×10 original concentration, was attained. Subsequently, the RO fouling test was performed with the concentrated test solution at flux of 20 L/m^2h and crossflow velocity of 0.10 m/s. Full recycle of retentate and permeate to the feed tank

was adopted to simulate the RO fouling at high recovery of 90%. The pH of test solution was maintained at pH 6.3 by acid dosing. The RO fouling test lasted for 5 days.

2.3. Analytical measurements

2.3.1. Water quality analysis

The feed water, mixed liquor and permeate of the NF-MBRs were sampled twice weekly for analysis. The supernatant of the feed water and mixed liquor was obtained by centrifuging for 10 min at 4000 ×g and then filtering through a 0.45 μm membrane filter before analysis. Total organic carbon (TOC) and total nitrogen (TN) were determined by a TOC/TN-V analyzer (Shimadzu, Japan). Chemical oxygen demand (COD), ammonia, nitrite, nitrate and total phosphorus were measured using the colorimetric method with a spectrophotometer (DR 3900, HACH, USA). Concentrations of cations were determined by an inductively coupled plasma optical emission spectrometry (ICP-OES, Optima 8000, Perkin Elmer, USA). The conductivity and total dissolved solids (TDS) were measured using a multi-function meter (Eutech Instruments, USA). Liquid chromatography-organic carbon detector (LC-OCD) analyzer (LC-OCD Model 8, DOC-LABOR, Germany), a size-exclusion chromatography system coupled with organic carbon detection and organic nitrogen detection was used to quantify the dissolved organic fractions according to their molecular weights (MWs): biopolymers (typically MW > 10 kDa), humic substances and building blocks (HS&BB, MW 350 – 1000 Da), low molecular weight organics (LMW, MW < 350 Da). Details of the LC-OCD system and analysis were described in the literature (Huber et al. 2011).

2.3.2. Biological analysis

The total solid amount in the bioreactor was defined as the sum of mixed liquor suspended solids (MLSS) and total attached solids on the bio-carriers. Similarly, the total biomass amount in the bioreactor was defined as the sum of mixed liquor volatile suspended solids (MLVSS) and total attached biomass on the bio-carriers. The attached solids/biomass on the bio-carrier was extracted by sonication (10 min) and vortex (1 min). The total attached solids/biomass was estimated by multiplying the attached solids/biomass amount extracted per bio-carrier (i.e., 2 pieces of biocarriers were sampled for analysis each time) with the total number of bio-carriers in the bioreactor. The total solids/biomass concentration was calculated by dividing the total solids/biomass amount by the effective reactor volume. The MLSS and MLVSS were measured according to Standard Methods (American Public Health et al. 2005). Particle size of the bioflocs was measured by a Mastersizer (MS2000, Malvern, UK). Zeta potential of the flocs was analyzed by a Zetasizer (ZEN3600, Malvern, UK).

The intracellular ATP (i.e., live cells) and extracellular ATP (i.e., dead cells) concentrations were measured according to manufacturer's specifications (Kikkoman, Japan). The viability of the activated sludge was determined by the ratio of intracellular ATP concentrations to the total ATP concentrations. The microbial activity was assessed by measuring the specific oxygen uptake rate (SOUR) of the activated sludge according to Standard Method 1683 (American Public Health et al. 2005).

The separation of bound EPS and soluble EPS in the mixed liquor and foulant solution was done by centrifuging the solution at 4000 ×g for 10 min at 4 °C. The supernatant was collected for soluble EPS measurement. The bound EPS was extracted by formaldehyde–NaOH method (Liu and Fang 2002, Zhang et al. 2006). Briefly, the solid fraction was re-suspended in

10 mL of ultrapure water, followed by adding 12 μL of formaldehyde (36.5%; Sigma Aldrich, USA) and keeping for 1 h at 4 °C. After that, 0.8 mL of 1M NaOH was added and kept for 3 h at 4 °C. Subsequently, the solution was centrifuged at 13200 ×g for 20 min and the supernatant was collected for bound EPS measurement. The EPS contents were determined by measurement of polysaccharides and proteins concentrations. The polysaccharides concentration was determined according to the phenol-sulfuric acid method with glucose as a standard and absorbance measurement at 490 nm using a spectrometer (HACH, USA) (Dubois et al., 1956). The protein concentration was determined by Bradford method with bovine serum albumin (BSA) as standard and absorbance measurement at 595 nm (Bradford 1976).

To examine the microbial community compositions, the suspended activated sludge samples in the NF-MBRs were collected during steady operation period and the cake layer foulants on NF2 membranes were collected at the end of operation. The genomic DNA of the microbial community was extracted from the samples by PowerSoil® DNA isolation kit (MO bio, USA). The 16S rRNA genes were sequenced by Illumina MiSeq platform using primers 357wF (CCTACGGGGNGGCWGCAG) and 785R (GACTACHVGGGTATCTAATCC). The sequencing results were analyzed by QIIME using the standard de novo operational taxonomic unit (OTU)-based approach.

2.3.3. NF membrane foulant solution preparation

At the end of NF-MBR operation, the fouled NF modules were removed for autopsy studies. The foulants were detached from the membrane surface (20 pieces of hollow fibers, 3 cm in length, total membrane area of 14.14 cm^2) by soaking the membrane in 20 mL of ultrapure water and ultra-sonicating for 30 min. The foulant solution (10 mL) was centrifuged at 4000 ×g for 10 min and then filtered through a 0.45 μm membrane filter. The supernatant (i.e., soluble

foulants) was collected for EPS and LC-OCD analysis. In addition, 10 mL of foulant solution was digested by adding 2% nitric acid. The digested foulant solution was centrifuged at 4000 ×g for 10 min and then filtered through a 0.45 μm membrane filter. The supernatant was collected for inorganic element analysis by ICP-OES.

2.3.4. Confocal laser scanning microscopy (CLSM)

CLSM (Leica, German) was employed to record the biofilm morphology after the membrane sample (1.3 mm × 0.45 mm) was stained with dyes. In detail, the biofilm on the membrane surface was stained with LIVE/DEAD BacLight™ Bacterial Viability kits (Molecular Probes, USA) according to manufacturer's instruction. The live and dead cells in the biofilm were analyzed and the biovolume was calculated using IMARIS software (version 7.1.3, Bitplane, Switzerland).

The EPS staining procedure was conducted according to a reported procedure (Adav et al. 2008). Briefly, 100 μL of 0.1M sodium bicarbonate buffer was added to the sample to maintain the amino groups in non-protonated status. Then 10 μL of 10 g/L fluorescein isothiocyanate (FITC, Molecular Probes, USA) solution was added to bind with proteins. The stained sample was placed on a shaker for 1 h. After that, 100 μL of 250 mg/L concanavalin A (Con A) conjugated with tetramethyl rhodamine (Molecular Probes, USA) was added to the sample to bind with α-d-glucopyranose-D polysaccharides and incubated at room temperature for 30 min. The stained sample was then washed twice with PBS to remove unbound dye. After that, 100 μL of 300 mg/L Calcofluor white (Sigma-Aldrich, USA) was added to the sample for 30 min to stain the β-polysaccharides and subsequently the sample was washed twice with PBS to remove excess dye. Lastly, 60 μL of 100 mg/L of Nile red (Molecular Probes, USA) was employed to bind with the intracellular lipids, followed by washing twice with PBS prior to CLSM analysis.

3. Results and Discussion

3.1. Impact of salt accumulation on NF-MBR performance

During 90-day operation of NF-MBRs, a gradual build-up and accumulation of scale-forming ions such as Ca, Mg, and PO_4, as well as TDS, DOC, and sCOD in the bioreactors was observed as expected due to their rejection by the NF membranes (Figure 1). The water quality of feed, mixed liquor ad permeate of NF-MBRs at steady state are summarized in Figure 2.

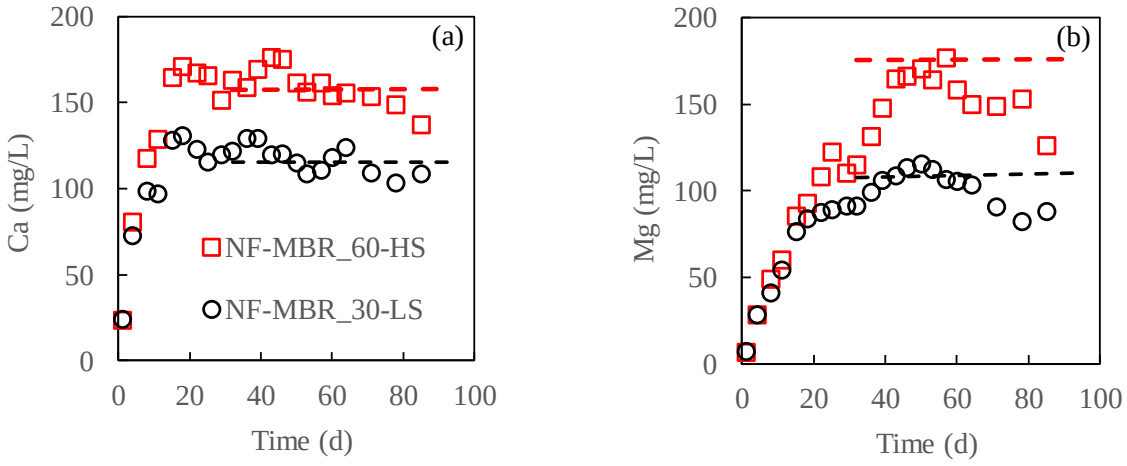

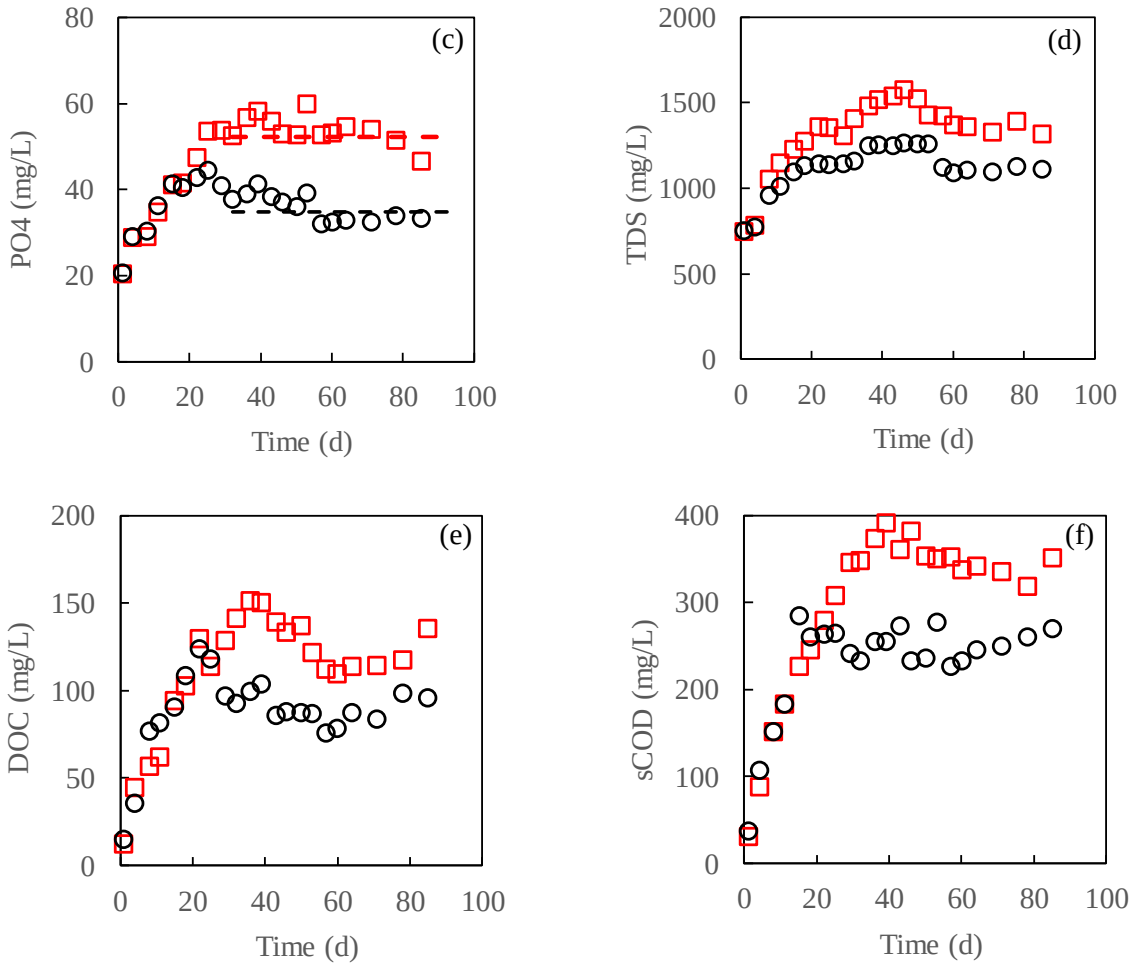

297 **Figure 1. (a) Ca, (b) Mg, (c) PO_4, (d) TDS, (e) DOC, and (f) sCOD in the mixed liquor of**

298 **NF-MBRs. Dotted-lines in the plot for Ca, Mg, PO_4 indicate the concentrations at steady**

299 **state as predicted by Eq. (1).**

300

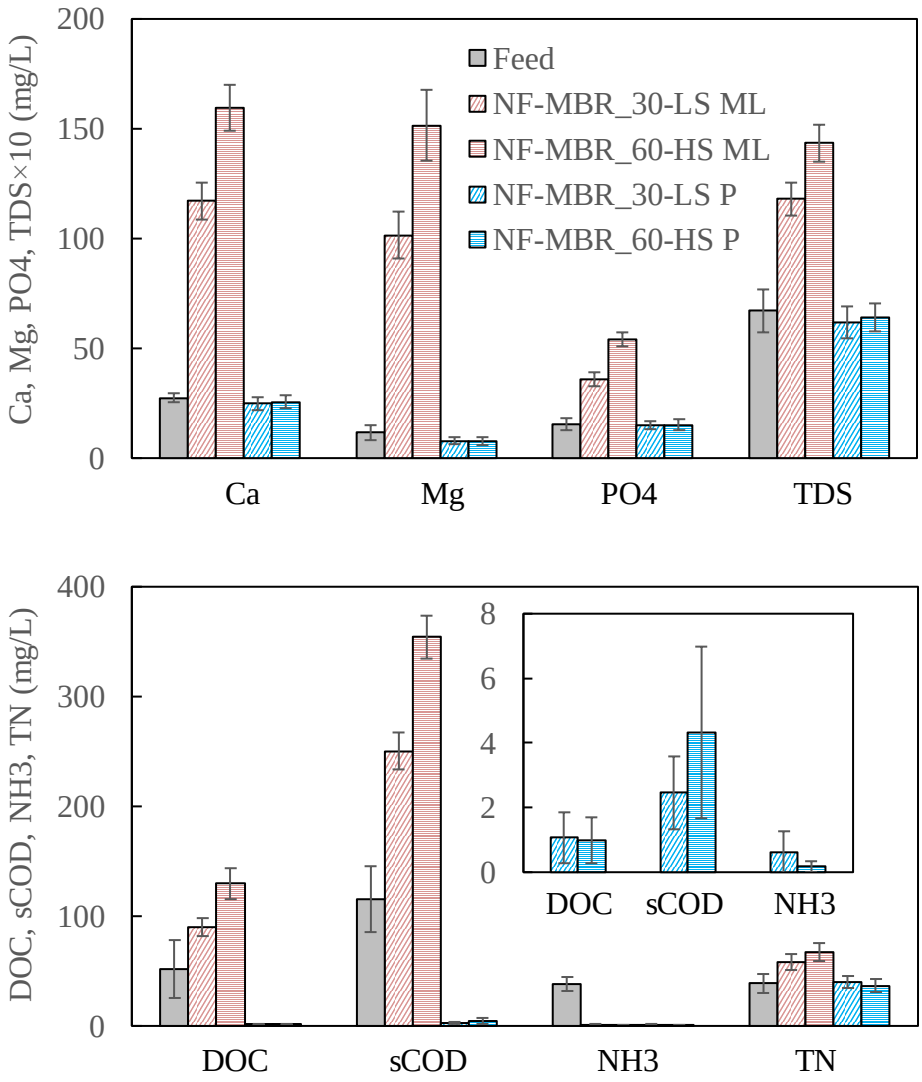

301

302 **Figure 2. Water quality of feed, mixed liquor, and permeate of NF-MBRs at steady state.**

303

304 Increasing the SRT, the measured concentrations of Ca (159.5±10.6 mg/L), Mg
305 (151.4±16.3 mg/L), PO_4 (53.9±3.3 mg/L), and TDS (1434.2±85.3 mg/L) in the mixed liquor of
306 NF-MBR_60-HS during steady state were approximately 36, 49, 51, and 22% higher than those
307 in the NF-MBR_30-LS (Ca at 116.9±8.3 mg/L, Mg at 101.4±10.7 mg/L, PO_4 at 35.7±3.1 mg/L,
308 and TDS at 1179.0±74.5 mg/L), respectively (Figure 1). To predict the mixed liquor salt
309 concentrations, C_{ml} at steady state, Eq. (1) was developed based on the mass balance of the NF-

MBR system which relates the SRT, HRT and NF membrane rejection, η_{NF} (refer to Appendix for details):

$$C_{ml}(t) = C_{\mathrm{f}}\left[\left(1 - \frac{1}{\alpha}\cdot\frac{1}{\mathrm{HRT}}\right)\cdot e^{-\alpha\cdot t} + \frac{1}{\alpha}\cdot\frac{1}{\mathrm{HRT}}\right] \text{ where } \alpha = \left[\left(\frac{1}{\mathrm{HRT}} - \frac{1}{\mathrm{SRT}}\right)(1-\eta_{\mathrm{NF}}) + \frac{1}{\mathrm{SRT}}\right] \quad \text{Eq. (1)}$$

Eq. (1) differs from the previous work that assumes the membrane (i.e., FO membrane) has perfect rejection (Lay et al. 2010). Eq. (1) assumes no salt precipitation in the bioreactor and scaling on the membrane surface, as well as no adsorption of inorganic ions onto the biomass or biofilm on the biocarriers. The measured concentrations correlated well within 15% error with the predicted concentrations, i.e., Ca = 115.3 and 157.7 mg/L, Mg = 108.6 and 175.6 mg/L, PO_4 = 34.8 and 52.2 mg/L for NF-MBR_30-LS and NF-MBR_60-HS, respectively. The discrepancies observed between the predicted and measured values could be due to these reasons.

Despite the good rejection properties of NF membrane, i.e., Ca = 79 - 84%, Mg = 92 - 95%, PO_4 = 58 - 72%, the overall removal attained for Ca, Mg, PO_4 was only <10, <35, and <2%, respectively, thus the NF-MBR permeate has almost similar concentrations of Ca and PO_4 as the incoming feed. Further optimization work such as chemical assisted precipitation is required to increase the removal efficiency. Tuning the NF membrane to get higher rejection, i.e., increase the number of polyelectrolyte layers or make a tighter membrane, is a complicated issue as on one hand excellent removal of divalent ions is desired but on the other hand increase rejection of monovalent ions can cause an increase in osmotic pressure.

The soluble organics in terms of DOC and sCOD in the mixed liquors also increased gradually before reaching steady values of DOC = 89.7±7.9 and 129.2±14.3 mg/L, sCOD =

250.1±17.1 and 354.1±19.7 mg/L for NF-MBR_30-LS and NF-MBR_60-HS, respectively (Figure 1). The accumulation of soluble organics in the NF-MBRs could be attributed to their rejections by the NF membrane and their slowly-biodegradable or non-biodegradable natures. Similar to inorganic ions, greater accumulation of soluble organics was found in the NF-MBR with longer SRT. The impact of salt accumulation on the biodegradation efficiency of NF-MBR can be assessed by estimating the biodegradation rate at steady state, which was defined as:

$$\text{biodegradation rate (\%)} = (1 - C_{ml,\ measured}/C_{ml,\ predicted}) \times 100\% \quad \text{Eq. (2)}$$

$C_{ml,\ measured}$ is the measured concentration of organics in the mixed liquor while $C_{ml,\ predicted}$ is the concentration of organics in the bioreactor assuming no biodegradation and negligible adsorption onto the membrane, which can be obtained using Eq. (1). The results showed that the biodegradation rate of DOC attained in NF-MBR_30-LS and NF-MBR_60-HS were ~92.0% ($C_{ml,\ predicted}$ = 1115.5 mg/L) and ~92.3% ($C_{ml,\ predicted}$ = 1679.8 mg/L), respectively, showing insignificant effect from salt accumulation at different SRT (p>0.05).

Both NF-MBRs produced permeates with comparable DOC contents (1.1±0.8 mg/L in NF-MBR_30-LS *vs.* 1.0±0.7 mg/L in NF-MBR_60-HS; p>0.05), achieving >97% of DOC removal (Figure 2). The NF-MBR_60-HS produced a permeate with slightly higher COD level compared to the NF-MBR_30-LS (4.3±2.7 mg/L *vs.* 2.5±1.1 mg/L; p<0.05). Nevertheless, both NF-MBRs could achieve COD removal of >99% (Figure 2). Not surprisingly, the superior permeate quality was owing to the excellent rejection properties of NF membranes toward organic matters, i.e., >98.5%, thus no obvious impact of salt accumulation on permeate quality in terms of DOC and sCOD could be observed, unlike in the case of dissolved ions. In addition, both NF-MBRs achieved excellent nitrification levels (ammonia removal ratios >98%) and

355 produced permeates with very low NH_3 levels (<1 mg/L) despite the elevated salinity condition
356 in the bioreactors. In contrast, the inhibition of nitrification process was commonly observed in
357 FO-MBR and MD-MBR due to the accumulation of NaCl (Qiu and Ting 2013, Wang et al. 2016,
358 Wijekoon et al. 2014). The nitrifiers responsible for the two-step bioprocess, i.e., ammonia
359 oxidizing bacteria (AOB) and nitrite oxidizing bacteria (NOB), are sensitive to high salt
360 environment (Campos et al. 2002, Moussa et al. 2006). In the NF-MBR system applied in this
361 study, the negative impact arisen from the accumulation of NaCl was alleviated by allowing the
362 passage of monovalent ions. Our findings suggested that the accumulation of Ca, Mg, and PO_4
363 has no adverse influence on the nitrification process.

364 The organic compositions of feed, mixed liquor, and permeate of NF-MBRs were
365 analyzed by LC-OCD (Table 3). In both NF-MBRs, it was observed that (1) NF membranes
366 demonstrated complete rejection of biopolymers, >99% rejection of HS&BB, and >95%
367 rejection of LWM; (2) HS&BB accounted for ~75% of total soluble organics in the bioreactors
368 compared to ~31% in the feed, indicating their larger accumulation rates, i.e., highest
369 concentration factor, due to their slowly-biodegradable or non-biodegradable nature; (3) Limited
370 accumulation of biopolymers (~10%) and LMW (~14%) in the bioreactors due to their easily-
371 biodegradable nature. In addition, the biodegradation rate of each fraction was estimated as
372 summarized in Table 3, and no obvious impact of salt accumulation was observed since both NF-
373 MBRs had similar biodegradation efficiencies for all components.

374

375 **Table 3. Compositions of soluble organics in the feed, mixed liquor, and permeate of NF-**
376 **MBRs analyzed by LC-OCD (n=5).**

	Biopolymers	HS&BB	LMW
Feed (mg/L)	5.2 ± 0.9	11.0 ± 4.9	18.9 ± 2.9

		(14.9%)	(31.1%)	(54.0%)
	Mixed Liquor (mg/L)	8.1 ± 0.5	55.3 ± 5.0	10.9 ± 1.5
		(10.3%)	(75.7%)	(14.0%)
NF-MBR_30-LS	CF[b]	1.55	5.02	0.57
	Biodegradation rate (%)	94.37	77.73	95.38
	Permeate (mg/L)	N.D.[a]	0.1 ± 0.0	0.5 ± 0.3
		(0%)	(14.3%)	(85.7%)
	Mixed Liquor (mg/L)	12.4 ± 2.3	83.5 ± 3.8	16.5 ± 2.3
		(11.0%)	(74.4%)	(14.6%)
NF-MBR_60-HS	CF	2.38	7.59	0.87
	Biodegradation rate (%)	94.13	75.81	94.21
	Permeate (mg/L)	N.D.	0.1 ± 0.0	0.4 ± 0.1
		(0%)	(20%)	(80%)

[a] N.D. represents not detectable;
[b] CF represents concentration factor, CF = C_{ml}/C_f.

3.2. Impact of salt accumulation on biomass characteristics

3.2.1. Short-term spike test

Short-term impact of rapid exposure of high concentration of divalent ions, i.e., relative to the feed concentration, on biomass characteristics was performed by spiking of salts into the bioreactors at different concentrations, namely control (no addition of salts), 200 and 400 mg/L Ca, 100 and 200 mg/L Mg. The physiological responses in terms of cell viability, microbial activity, and EPS production on Day 0, 4 and 7 are summarized in Figure S3 (Appendix). Interestingly, the abrupt change in salt concentrations did not show any negative impact on the biomass characteristics. As compared to control, the addition of Ca increased the viability of biomass by 52 and 33% for 200 and 400 mg/L Ca, respectively, whereas no changes for samples spiked with Mg. In addition, the microbial activity as reflected by SOUR analysis showed 29% increase at 200 mg/L Ca while no notable change for 400 mg/L Ca, 100 and 200 mg/L Mg. The

392 improved viability and SOUR could be attributed to the important role of calcium ions in
393 maintaining the cell structure, cell division, and signal transduction that subsequently promote
394 cell growth and increase microbial activity (Dominguez 2004, Yu and Margolin 1997).
395 Furthermore, the EPS production was increased by 35 and 34% when spiked with 100 and 200
396 mg/L Mg, respectively, but comparable EPS production as control when spiked with 200 and
397 400 mg/L Ca, which indicated an increase in Ca had negligible impact on EPS production in NF-
398 MBRs.

399 *3.2.2. Microbial activity and viability*

400 The characteristics of biomass in mixed liquor (i.e., suspended biomass) and on
401 biocarriers (i.e., attached biomass) during long term operation of NF-MBRs, i.e., gradual
402 accumulation of salts until steady state, are summarized in Table 4. The average MLSS (i.e., total
403 suspended solids) concentrations in NF-MBR_30-LS and NF-MBR_60-HS were relatively
404 comparable at 1277±286 mg/L and 1282±240 mg/L (p>0.05), respectively. In contrast, the
405 attached solids on biocarriers of NF-MBR_60-HS (594±132 mg/L) was higher than NF-
406 MBR_30-LS (515±134 mg/L; p<0.05), leading to a higher total solids amount (p<0.05). Both
407 NF-MBRs also had similar MLVSS/MLSS ratio (0.79-0.89; p>0.05). The viability and activity
408 of the suspended biomass were examined by ATP and SOUR analysis (Table 5). In both NF-
409 MBRs, the viability increased gradually with time, but SOUR maintained relatively constant
410 (Figure S4 in Appendix). Averagely, in NF-MBR_30-LS, the biomass had viable ratio of 59±9%
411 and SOUR of 11.2±1.9 mgO_2/gMLVSS·h, whereas the viability and SOUR in NF-MBR_60-HS
412 were 60±12% and 12.4±2.4 mgO_2/gMLVSS·h, p> 0.05, respectively. Although the viability and
413 SOUR in NF-MBR_60-HS were slightly higher, the values were not statistically significant,

414 suggested that the impact of Ca accumulation was not remarkable in the long-term operation of
415 NF-MBR.

416 *3.2.3. EPS production*

417 In addition, the soluble and bound EPS productions of suspended biomass in both NF-
418 MBRs experienced increase during initial stage, followed by slow decrease, regardless of SRT
419 (Figure S5 in Appendix). The results agreed with the spike test above, which showed Mg had
420 greater impact on EPS production. It was also noted that soluble EPS accounted for almost 50%
421 of the total EPS in our NF-MBRs and such ratio was higher than those reported in conventional
422 MBRs (Wu et al. 2011, Zhang et al. 2010). Table 4 further compares the compositions of EPS
423 (i.e., polysaccharides and protein) in both NF-MBRs at steady state. The amount of protein was
424 almost three folds of polysaccharides for both soluble and bound EPS, regardless of the SRT. In
425 addition, higher soluble polysaccharides (i.e., ~35%) were present in NF-MBR_60-HS than NF-
426 MBR_30-LS (p<0.05), while comparable soluble proteins were found in both NF-MBRs
427 (p>0.05). Both NF-MBRs produced comparable amount of bound proteins (p>0.05) and bound
428 polysaccharides (p>0.05). The results suggested that SRT could influence soluble EPS
429 production in NF-MBRs, especially soluble polysaccharides.

430 *3.2.4. Particle size and zeta potential*

431 Furthermore, the suspended biomass in NF-MBR_60-HS had larger floc sizes (p<0.05)
432 and less negative surface charges (p<0.05) compared to those in NF-MBR-30-LS, (Table 4). This
433 could be attributed to the presence of higher concentrations of divalent cations under longer
434 SRT, which enhanced the bridging between negatively-charged functional groups of the bioflocs,
435 in particular the charge neutralization effect and decrease in zeta potential to become less
436 negative was more pronounced for Ca (Sobeck and Higgins 2002, Zhang et al. 2016). It has been

reported that bioflocculation could be beneficial to membrane fouling reduction in conventional MBRs (Van den Broeck et al. 2012), its impact in NF-MBRs will be discussed in Section 3.3.

Table 4. Characteristics of biomass in NF-MBRs (n=11).

Biomass characteristics		NF-MBR_30-LS	NF-MBR_60-HS
Attached biomass	Total solids (mg/L)	515±134	594±132
	Total biomass (mg/L)	453±117	515±107
Suspended biomass	Total solids (MLSS) (mg/L)	1277±286	1282±240
	Total biomass (MLVSS) (mg/L)	1084±274	1061±223
	Viability (%)	59±9	60±12
	SOUR (mgO_2/gMLVSS·h)	11.2±1.9	12.4±2.4
	Soluble protein (mg/gMLVSS)	56±10	63±9
	Soluble polysaccharides (mg/gMLVSS)	23±5	31±4
	Bound protein (mg/gMLVSS)	69±7	70±10
	Bound polysaccharides (mg/gMLVSS)	23±6	25±4
	Particle size (μm)	95±4	114±5
	Zeta potential (mV)	-11.7±0.8	-9.9±1.0

3.2.5. Microbial community

In addition, the microbial community compositions and relative abundances of bacterial populations at phylum level of suspended activated sludge in both NF-MBRs are illustrated in Figure 3. It was found that at phylum level, Proteobacteria (48.7% in NF-MBR_30-LS *vs.* 51.2% in NF-MBR_60-HS) and Planctomycetes (15.7% in NF-MBR_30-LS *vs.* 14.9% in NF-MBR_60-HS) were the predominant microbial communities. This observation was similar to the reported findings in conventional MBRs (Jo et al. 2016, Takimoto et al. 2018, Xia et al. 2012). Also, the microbial communities in both NF-MBRs had comparable relative abundances (Figure

3) with similar observed OTU, Chao1, Shannon and Simpson diversity indexes (Table 5). It implied that the microbial communities in NF-MBRs were not significantly affected by the increased organic and salt accumulations with extending SRT.

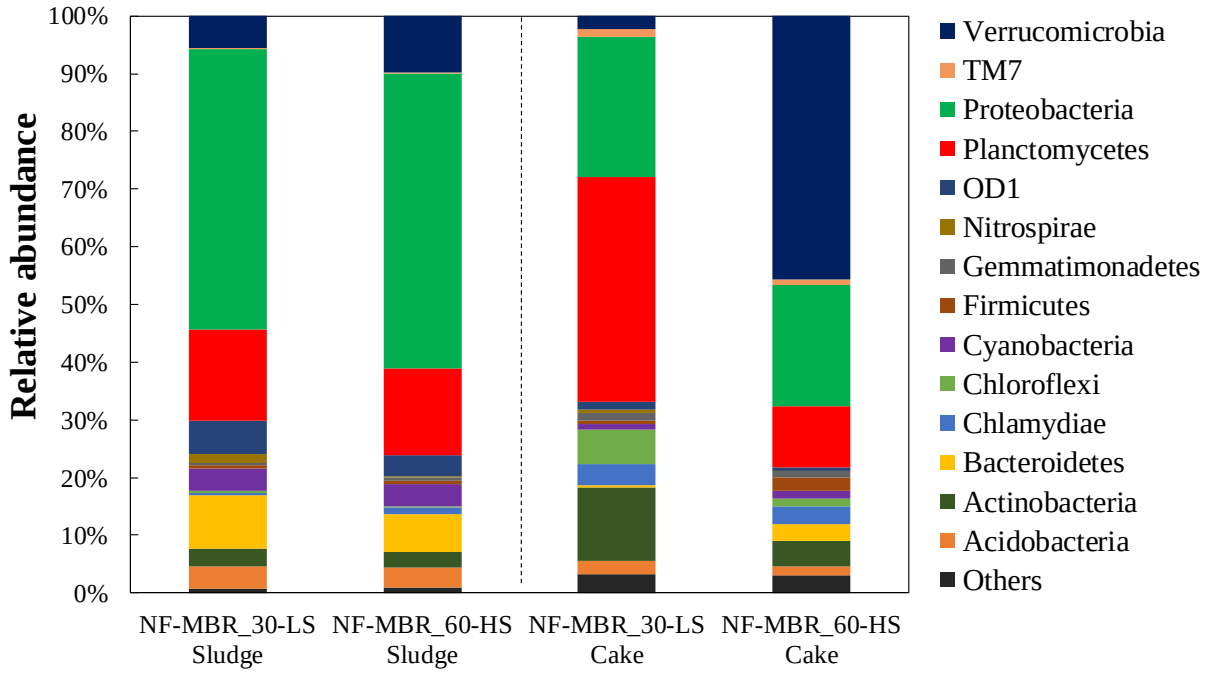

Figure 3. Prokaryotic community compositions of activated sludge and cake layers from NF membranes at the phylum level. All classified taxa with relative abundance lower than 1% and unclassified taxa were assigned to "Others".

Table 5. The observed OTU, Chao1, Shannon and Simpson diversity indexes of prokaryotic communities in NF-MBRs.

Sample	Observed OTU	Chao1	Shannon	Simpson
NF-MBR_30-LS sludge	555	585.9	4.129	0.943
NF-MBR_60-HS sludge	635	659.5	4.165	0.940
NF-MBR_30-LS cake	791	829.7	5.095	0.983

NF-MBR_60-HS cake	349	361	3.424	0.821

464

465 3.3. Impact of salt accumulation on NF membrane fouling

466 *3.3.1. TMP and permeability of NF-MBRs*

467 Figure 4a describes the TMP profile of NF-MBRs. During initial stage of operation
468 before the NF-MBRs reached steady operation and without applying the sponge column (from
469 Day 0 to 30, NF1), severe fouling accompanied by rapid increase in TMP was observed due to
470 high loading of bioflocs directly to the NF module, i.e., clogging of lumen. Hence, the discussion
471 will be focused on the later stages (II, III and IV) of operation for NF2. In general, the TMP
472 profile displayed a 'sawtooth' pattern, in particular during stage III and IV, which was associated
473 with the interplay between reversible, irreversible fouling and cake-enhanced osmotic pressure
474 effect (CEOP) (Tay et al. 2018). To further examine the NF membrane fouling mechanisms, the
475 irreversible fouling resistance, $R_{irr}(t)$, $\Delta TMP_t = (TMP(t) - TMP(0))$ and $\Delta TMP_{irr} = J\mu R_{irr}(t)$, as
476 shown in Figure 4b and c, were calculated from the clean membrane pure water permeability,
477 membrane pure water permeability after each physical cleaning cycle (Figure S6) and TMP
478 profile (Figure 4a) according to the model developed in our previous publication (refer to
479 Appendix) (Tay et al. 2018). During Stage II operation, at backwashing pressure of 2 bar and
480 flushing crossflow velocity of 0.5 m/s, there was an initial slow build-up (i.e., first 10 days of
481 operation of NF2) followed by an exponential increase of irreversible fouling, where R_{irr} = ~20
482 and 30 × 10^{12} m^{-1} after 25 days of operation of NF2 for NF-MBR_30-LS and NF-MBR_60-HS,
483 respectively. In Stage III, the flushing crossflow velocity was increased from 0.5 m/s to 0.8 m/s
484 with a fixed backwashing pressure of 2 bar in order to improve the cleaning efficiency, where the
485 R_{irr} dropped to 12 and 27 × 10^{12} m^{-1} for NF-MBR_30-LS and NF-MBR_60-HS, respectively.
486 The cleaning protocol appeared to be effective for the case of NF-MBR_30-LS as it prevented

further increase in R_{irr}, but not for the case of NF-MBR_60-HS as there was a linear (average) increase in R_{irr}. In Stage IV, the backwashing pressure was increased from 2 to 3 bar with a fixed flushing crossflow velocity of 0.8 m/s, but it did not further remove the irreversible fouling for NF-MBR_30-LS, only maintained R_{irr} at the same level. Meanwhile, the R_{irr} continued to increase linearly (average) for NF-MBR_60-HS, hence physical cleaning was not effective in this case. These observations implied that the cake layer morphology in NF-MBRs may be different (×3.5 higher in final R_{irr} value), i.e., more compact cake layer in NF-MBR_60-HS compared to NF-MBR_30-LS, as a result of salt accumulation effect (discussed below). In addition, chemical cleaning was performed using citric acid after 43 and 52 days of operation of NF2 for both NF-MBRs. Apparently, the membrane permeability of NF-MBR_60-HS could be restored by ~12-42%, suggesting partial irreversible fouling was removed by chemical cleaning. However, the effect of chemical cleaning in NF-MBR_30-LS was not remarkable (<5% restoration), indicating the limitations of chemical cleaning using citric acid in the restoration of membrane permeability. Therefore, further optimization of chemical cleaning protocol is crucially important in future studies on NF-MBR. The NF membrane (layer-by-layer polyelectrolytes of PAH and PSS) used in this work cannot tolerate pH>8, one option is to apply chemical-enhanced backwashing with weak acid, EDTA, or SDS (Lateef et al. 2013).

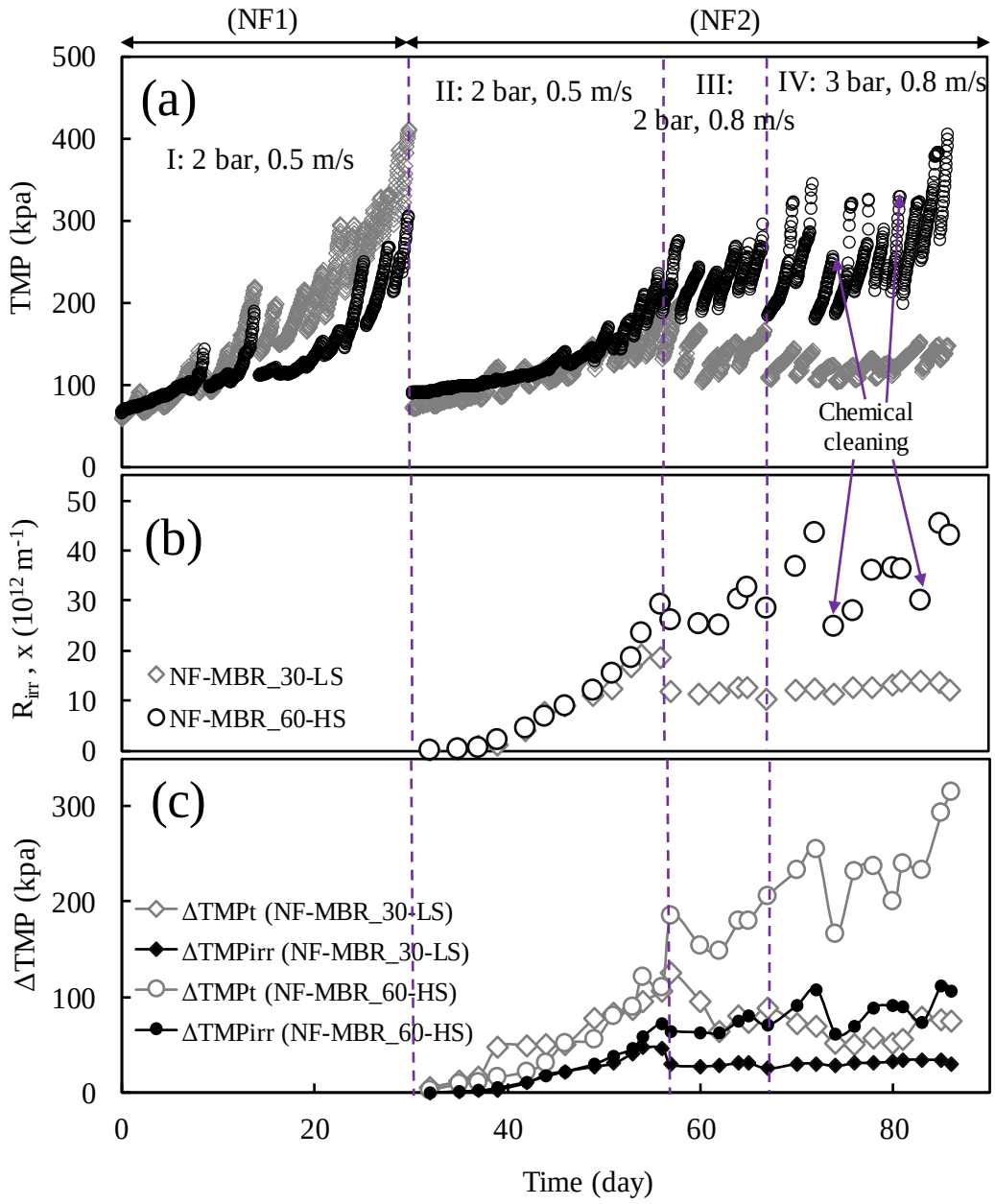

Figure 4. (a) TMP profile, (b) Irreversible fouling resistance, R_{irr}, and (c) ΔTMP_t and ΔTMP_{irr} for NF-MBRs.

The CEOP effect, approximated by $\Delta TMP_{CEOP} \approx (\Delta TMP_t - \Delta TMP_{irr})$, is associated with the cake thickness, porosity and tortuosity (Chong et al. 2008). Therefore, there was no immediate and sharp rise in TMP (i.e., the upward part of the 'sawtooth') during initial stage

511 (first 10 days) of NF2 operation, but an obvious TMP increase was noticed when a substantial
512 cake layer was formed during later stage in Stage II as well as throughout Stage III and IV. As
513 shown in Figure 4c, the CEOP effect was the predominant contributor and more severe in TMP
514 increase for NF-MBR_60-HS, which was attributed to the thicker and more compact cake layer
515 as well as higher salt concentration (i.e., osmotic pressure), as compared to NF-MBR_30-LS.

516 *3.3.2. NF membrane foulants*

517 (1) Morphology of cake layer foulants

518 The CLSM images of cells (live cells and dead cells) and EPS (proteins, α-d-
519 glucopyranose-D polysaccharides, β-polysaccharides and intracellular lipids) are shown in
520 Figure 5 and the calculated biovolumes are summarized in Table 6. The biovolumes of live cells
521 (predominantly present on the cake layer surface), dead cells (abundantly distributed in both
522 inner and outer regions of the cake layers), and total EPS in the NF foulants of NF-MBR_60-HS
523 were higher than NF-MBR_30-LS. First, the higher amount of live cells and EPS production
524 were due to greater availability of DOC and no inhibition of salt accumulation to support the
525 biofilm formation. Second, the higher amount of EPS, especially polysaccharides, was associated
526 with the greater amount of Ca that formed polysaccharides-Ca complex with strong gelation
527 properties (Meng et al. 2011), which could not be easily removed by physical cleaning. Third,
528 the higher amount of dead cells could be due to the greater operating pressure, which led to the
529 formation of a compact cake layer that hindered the oxygen and nutrient transfer to the inner
530 region of cake layer.

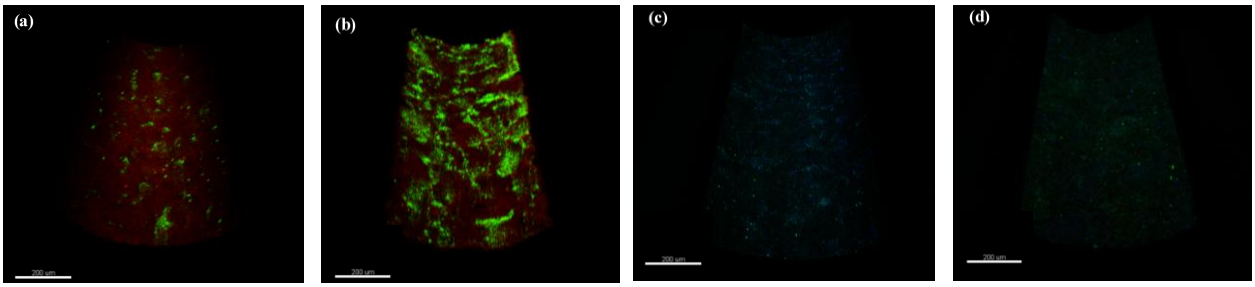

Figure 5. CLSM images of cake layer foulants on NF membranes. Images of live/dead cells in (a) NF-MBR_30-LS and (b) NF-MBR_60-HS; Images of proteins (FITC), α-d-glucopyranose polysaccharides (Con A), β-polysaccharides (calcofluor white), and intracellular lipids (Nile red) in (c) NF-MBR_30-LS and (d) NF-MBR_60-HS.

Table 6. Characteristics of cake layer foulants on NF membranes in NF-MBRs (n=2).

Foulants characteristics		NF-MBR_30-LS	NF-MBR_60-HS
CLSM image analysis	Live cells ($\mu m^3/\mu m^2$)	0.23 ± 0.02	1.75 ± 0.07
	Dead cells ($\mu m^3/\mu m^2$)	0.93 ± 0.43	1.69 ± 0.11
	Protein (10^5 $\mu m^3/cm^2$)	2.86 ± 0.18	2.72 ± 0.22
	α-d-glucopyranose polysaccharides (10^5 $\mu m^3/cm^2$)	3.36 ± 2.10	29.23 ± 11.34
	β-polysaccharides (10^5 $\mu m^3/cm^2$)	8.77 ± 3.33	34.27 ± 7.7
	Intracellular lipids (10^5 $\mu m^3/cm^2$)	N.D.[a]	N.D.
LC-OCD analysis	Biopolymers (mg/m^2)	200.6 ± 10.3	305.5 ± 21.5
	HS & BB (mg/m^2)	93.1 ± 11.4	235.36 ± 22.4
	LMW (mg/m^2)	31.8 ± 1.1	57.1 ± 3.0
ICP-OES analysis	Ca (mg/m^2)	160.6 ± 21.6	226.1 ± 14.1
	Mg (mg/m^2)	49.2 ± 2.7	97.6 ± 7.1
	P (mg/m^2)	103.0 ± 13.2	142.2 ± 31.5
	S (mg/m^2)	30.0 ± 20.6	48.8 ± 37.8
	Si (mg/m^2)	21.0 ± 12.4	19.1 ± 5.4

[a] N.D. represents "not detectable".

(2) Organic compositions

In both NF-MBRs, the biopolymers appeared to be the predominant species, accounting to 51-61%. The results agreed well with our previous study on NF-MBRs operated at different conditions (Tay et al. 2018). The organic fractions (i.e., biopolymers, HS&BB, and LMW) in the cake layer foulants of NF-MBR_60-HS were greater than NF-MBR_30-LS. Possibly, this was due to more adsorption from the higher concentration in the bulk solution as well as more dead cell lysis in the cake layer biofilm.

(3) Inorganic compositions

Higher accumulations of Ca (226.1 mg/m^2), Mg (97.6 mg/m^2), P (173.6 mg/m^2), S (48.8 mg/m^2), and Si (19.1 mg/m^2) were found on the NF membrane in NF-MBR_60-HS (vs. Ca of 160.8 mg/m^2, Mg of 49.2 mg/m^2, P of 103.0 mg/m^2, S of 30.0 mg/m^2, and Si of 21.0 mg/m^2 for NF-MBR_30-LS) owing to the higher concentrations of salts in the mixed liquor, in particular, calcium phosphate accounted for more than 60% of total inorganic foulants on the NF membranes. Note that the solubility limit of $Ca_3(PO_4)_2$, i.e. 2.07×10^{-33}, has been far exceeded in the bioreactors (refer to Appendix).

(4) Microbial community compositions

In the cake layer foulants of NF-MBR_30-LS, Planctomycetes and Proteobacteria were the dominant phyla, accounting for 38.9% and 24.4%, respectively (Figure 4), similar to conventional aerobic MBRs (Chen et al. 2016). In contrast, the dominant microbial community in the cake layer foulants of NF-MBR_60-HS was Verrucomicrobia (45.7%), which showed a low relative abundance in the suspended activated sludge (Figure 3). It has been reported that Verrucomicrobia has the ability to hydrolyze high-molecular-weight substrates such as polysaccharides (Cardman et al. 2014). Nevertheless, it suggested that salt accumulation could

affect the composition of microbial communities in the cake layer foulants of NF-MBRs. In addition, the observed OTU and Chao1, Shannon, and Simpson diversity indexes of microbial communities in the cake layers of NF-MBR_60-HS were 55.9%, 56.5%, 32.8%, and 16.5% lower than NF-MBR_30-LS, respectively (Table 5). The differences in microbial community structure may be attributed to factors, such as operating pressure (Gao et al. 2013), compositions and contents of EPS on the membrane surface (Tsuneda et al. 2003).

3.4. Impact of salt accumulation in NF-MBRs on performance of downstream RO membranes

As shown in Figure 6, during the concentration stage (i.e., when recovery was increased from 0 to 90%), the TMP increased from ~5.3 to 7.5 and 8.5 bar; while during continuous operation at recovery equivalent to 90%, the fouling rates (i.e., dTMP/dt) were ~0.25 and ~0.38 bar/d for RO fed with permeate of NF-MBR_30-LS and NF-MBR_60-HS, respectively. In conventional MF/UF-MBR+RO systems, it had been demonstrated that the higher organic levels (in terms of TOC, COD, EPS) in MBR permeate could lead to more serious RO membrane fouling (Wu et al. 2013). However, in this study, the permeates of both NF-MBRs had comparable quality (except higher sCOD for permeate of NF-MBR_60-HS), but resulted in relatively higher fouling rate for permeate of NF-MBR_60-HS. In addition, previous studies had emphasized that assimilable organic carbon (AOC) was an important parameter in determining the biofouling potential of RO feed water in seawater desalination (Lee et al. 2019, Wu et al. 2017), which had very low DOC concentration (< 2 mg/L) similar to the permeate of NF-MBR. Therefore, it was unclear the difference in fouling rate was due the difference in sCOD level or rather the compositions of organics. Further study will be focused on the effect of AOC in NF-MBR permeate on RO membrane performance in order to further advance the NF-MBR+RO for water reclamation.

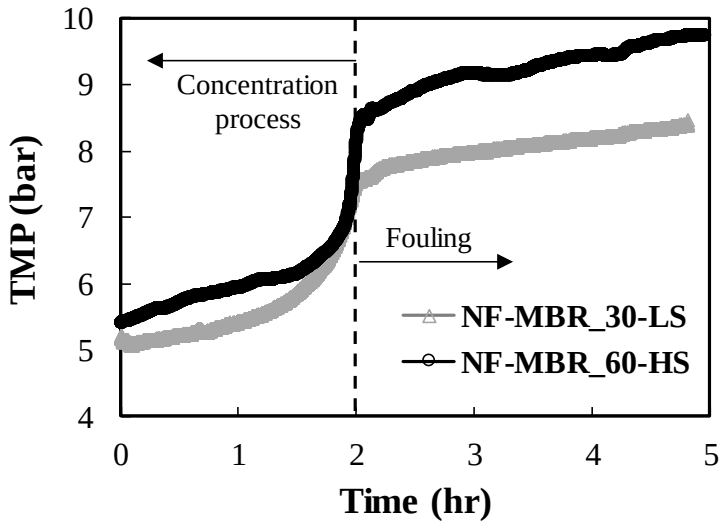

585

586 **Figure 6. Performance of RO fed with different NF-MBR permeates.**

587

588 **4. Conclusions**

589 This study compared the bioreactor and membrane performances in parallel NF-
590 MBR+RO systems for water reclamation application under different salt accumulation
591 conditions in NF-MBRs, which were operated under SRT of 30 and 60 days, respectively. The
592 following conclusions can be drawn:

593 (1) The concentration factor is a function of SRT, HRT and membrane rejection. Increasing the
594 SRT resulted in greater accumulation of scale-forming inorganic salts (i.e., Ca, Mg, PO_4) and
595 organic compounds (i.e., DOC, sCOD, and especially HS&BB due to its poor or non-
596 biodegradable nature). The accumulation of divalent ions did not pose adverse impact to the
597 biodegradation efficiency and both NF-MBRs achieved superior organic removal (>97%) and
598 ammonia removal (>98%).

599 (2) The elevated divalent ions level promoted bioflocculation, however, the effects on microbial
600 activity and viability were not statistically significant in the long-term experiment. Salt

accumulation did not influence the microbial community structure of activated sludge in NF-MBRs, but led to different predominant microbial communities in the cake layer foulants of NF membranes.

(3) More severe membrane fouling in the NF-MBR at longer SRT (i.e., higher salt accumulation) due to combined organic and inorganic fouling by calcium phosphate scaling and Ca-polysaccharides complex that was not easily removed by physical cleaning. The thicker and more compact irreversible fouling layer as well as higher salt concentration caused more severe cake-enhanced osmotic pressure (CEOP) effect in the NF-MBR with longer SRT. Physical cleaning (i.e., backwash and flushing) can be applied to maintain sustainable operation of the NF-MBR at low SRT of 30 d.

(4) Higher RO membrane fouling rate was observed when fed with permeate of NF-MBR with longer SRT, despite having similar water quality, i.e., DOC of <2 mg/L. One possible explanation was the role of AOC towards RO fouling at low DOC level, which required further investigation in future studies.

Acknowledgements

This research grant is supported by the Singapore National Research Foundation under its Urban Solution & Sustainability Programme and administered by PUB, Singapore's National Water Agency. The funding support from the Economic Development Board (EDB) of Singapore to the Singapore Membrane Technology Centre (SMTC) is also acknowledged.

References

Adav, S.S., Lee, D.J. and Tay, J.H. (2008) Extracellular polymeric substances and structural stability of aerobic granule. Water Research 42(6-7), 1644-1650.

American Public Health, A., Eaton, A.D., American Water Works, A. and Water Environment, F. (2005) Standard methods for the examination of water and wastewater, APHA-AWWA-WEF, Washington, D.C.
Bradford, M.M. (1976) A rapid and sensitive method for the quantitation of microgram quantities of protein utilizing the principle of protein-dye binding. Analytical Biochemistry 72(1), 248-254.
Campos, J.L., Mosquera-Corral, A., Sánchez, M., Méndez, R. and Lema, J.M. (2002) Nitrification in saline wastewater with high ammonia concentration in an activated sludge unit. Water Research 36(10), 2555-2560.
Cardman, Z., Arnosti, C., Durbin, A., Ziervogel, K., Cox, C., Steen, A.D. and Teske, A. (2014) Verrucomicrobia are candidates for polysaccharide-degrading bacterioplankton in an arctic fjord of Svalbard. Appl Environ Microbiol 80(12), 3749-3756.
Chen, F., Bi, X. and Ng, H.Y. (2016) Effects of bio-carriers on membrane fouling mitigation in moving bed membrane bioreactor. Journal of Membrane Science 499, 134-142.
Choi, J.-H., Fukushi, K., Ng, H.Y. and Yamamoto, K. (2006) Evaluation of a long-term operation of a submerged nanofiltration membrane bioreactor (NF MBR) for advanced wastewater treatment. Water Science and Technology 53(6), 131-136.
Choi, J.-H., Lee, S.H., Fukushi, K. and Yamamoto, K. (2007) Comparison of sludge characteristics and PCR–DGGE based microbial diversity of nanofiltration and microfiltration membrane bioreactors. Chemosphere 67(8), 1543-1550.
Chong, T.H., Wong, F.S. and Fane, A.G. (2008) Implications of critical flux and cake enhanced osmotic pressure (CEOP) on colloidal fouling in reverse osmosis: Experimental observations. Journal of Membrane Science 314(1), 101-111.
Colt, J. (2012) Computation of Dissolved Gas Concentration in Water as Functions of Temperature, Salinity and Pressure (Second Edition). Colt, J. (ed), pp. 73-131, Elsevier, London.
Dominguez, D.C. (2004) Calcium signalling in bacteria. Molecular Microbiology 54(2), 291-297.
Gao, D., Fu, Y. and Ren, N. (2013) Tracing biofouling to the structure of the microbial community and its metabolic products: A study of the three-stage MBR process. Water Research 47(17), 6680-6690.
Ge, S., Wang, S., Yang, X., Qiu, S., Li, B. and Peng, Y. (2015) Detection of nitrifiers and evaluation of partial nitrification for wastewater treatment: A review. Chemosphere 140, 85-98.
Huber, S.A., Balz, A., Abert, M. and Pronk, W. (2011) Characterisation of aquatic humic and non-humic matter with size-exclusion chromatography – organic carbon detection – organic nitrogen detection (LC-OCD-OND). Water Research 45(2), 879-885.
Iorhemen, O.T., Hamza, R.A. and Tay, J.H. (2017) Membrane fouling control in membrane bioreactors (MBRs) using granular materials. Bioresource Technology 240, 9-24.
Jo, S.J., Kwon, H., Jeong, S.-Y., Lee, C.-H. and Kim, T.G. (2016) Comparison of microbial communities of activated sludge and membrane biofilm in 10 full-scale membrane bioreactors. Water Research 101, 214-225.
Lateef, S.K., Soh, B.Z. and Kimura, K. (2013) Direct membrane filtration of municipal wastewater with chemically enhanced backwash for recovery of organic matter. Bioresource Technology 150, 149-155.
Lay, W.C.L., Liu, Y. and Fane, A.G. (2010) Impacts of salinity on the performance of high retention membrane bioreactors for water reclamation: A review. Water Research 44(1), 21-40.

Lee, S., Suwarno, S.R., Quek, B.W.H., Kim, L., Wu, B. and Chong, T.H. (2019) A comparison of gravity-driven membrane (GDM) reactor and biofiltration plus GDM reactor for seawater reverse osmosis desalination pretreatment. Water Research 154, 72-83.
Liu, C., Shi, L. and Wang, R. (2015) Crosslinked layer-by-layer polyelectrolyte nanofiltration hollow fiber membrane for low-pressure water softening with the presence of SO42− in feed water. Journal of Membrane Science 486, 169-176.
Liu, H. and Fang, H.H.P. (2002) Extraction of extracellular polymeric substances (EPS) of sludges. Journal of Biotechnology 95(3), 249-256.
Luján-Facundo, M.J., Fernández-Navarro, J., Alonso-Molina, J.L., Amorós-Muñoz, I., Moreno, Y., Mendoza-Roca, J.A. and Pastor-Alcañiz, L. (2018) The role of salinity on the changes of the biomass characteristics and on the performance of an OMBR treating tannery wastewater. Water Research 142, 129-137.
Luo, W., Hai, F.I., Price, W.E., Guo, W., Ngo, H.H., Yamamoto, K. and Nghiem, L.D. (2014) High retention membrane bioreactors: Challenges and opportunities. Bioresource Technology 167, 539-546.
Massé, A., Spérandio, M. and Cabassud, C. (2006) Comparison of sludge characteristics and performance of a submerged membrane bioreactor and an activated sludge process at high solids retention time. Water Research 40(12), 2405-2415.
Meng, F., Zhou, Z., Ni, B.-J., Zheng, X., Huang, G., Jia, X., Li, S., Xiong, Y. and Kraume, M. (2011) Characterization of the size-fractionated biomacromolecules: Tracking their role and fate in a membrane bioreactor. Water Research 45(15), 4661-4671.
Moussa, M.S., Sumanasekera, D.U., Ibrahim, S.H., Lubberding, H.J., Hooijmans, C.M., Gijzen, H.J. and van Loosdrecht, M.C.M. (2006) Long term effects of salt on activity, population structure and floc characteristics in enriched bacterial cultures of nitrifiers. Water Research 40(7), 1377-1388.
Nawaz, M.S., Gadelha, G., Khan, S.J. and Hankins, N. (2013) Microbial toxicity effects of reverse transported draw solute in the forward osmosis membrane bioreactor (FO-MBR). Journal of Membrane Science 429, 323-329.
Ng, H.Y., Tan, T.W. and Ong, S.L. (2006) Membrane Fouling of Submerged Membrane Bioreactors: Impact of Mean Cell Residence Time and the Contributing Factors. Environmental Science & Technology 40(8), 2706-2713.
Phan, H.V., McDonald, J.A., Hai, F.I., Price, W.E., Khan, S.J., Fujioka, T. and Nghiem, L.D. (2016) Biological performance and trace organic contaminant removal by a side-stream ceramic nanofiltration membrane bioreactor. International Biodeterioration & Biodegradation 113, 49-56.
Pollice, A., Laera, G. and Blonda, M. (2004) Biomass growth and activity in a membrane bioreactor with complete sludge retention. Water Research 38(7), 1799-1808.
Qiu, G. and Ting, Y.-P. (2013) Osmotic membrane bioreactor for wastewater treatment and the effect of salt accumulation on system performance and microbial community dynamics. Bioresource Technology 150, 287-297.
Sobeck, D.C. and Higgins, M.J. (2002) Examination of three theories for mechanisms of cation-induced bioflocculation. Water Research 36(3), 527-538.
Suwarno, S.R., Hanada, S., Chong, T.H., Goto, S., Henmi, M. and Fane, A.G. (2016) The effect of different surface conditioning layers on bacterial adhesion on reverse osmosis membranes. Desalination 387, 1-13.

Takimoto, Y., Hatamoto, M., Ishida, T., Watari, T. and Yamaguchi, T. (2018) Fouling Development in A/O-MBR under Low Organic Loading Condition and Identification of Key Bacteria for Biofilm Formations. Scientific Reports 8(1), 11427.
Tay, M.F., Liu, C., Cornelissen, E.R., Wu, B. and Chong, T.H. (2018) The feasibility of nanofiltration membrane bioreactor (NF-MBR)+reverse osmosis (RO) process for water reclamation: Comparison with ultrafiltration membrane bioreactor (UF-MBR)+RO process. Water Research 129, 180-189.
Tsuneda, S., Aikawa, H., Hayashi, H., Yuasa, A. and Hirata, A. (2003) Extracellular polymeric substances responsible for bacterial adhesion onto solid surface. FEMS microbiology letters 223(2), 287-292.
Van den Broeck, R., Van Dierdonck, J., Nijskens, P., Dotremont, C., Krzeminski, P., van der Graaf, J.H.J.M., van Lier, J.B., Van Impe, J.F.M. and Smets, I.Y. (2012) The influence of solids retention time on activated sludge bioflocculation and membrane fouling in a membrane bioreactor (MBR). Journal of Membrane Science 401-402, 48-55.
Wang, X., Chang, V.W.C. and Tang, C.Y. (2016) Osmotic membrane bioreactor (OMBR) technology for wastewater treatment and reclamation: Advances, challenges, and prospects for the future. Journal of Membrane Science 504, 113-132.
Wijekoon, K.C., Hai, F.I., Kang, J., Price, W.E., Guo, W., Ngo, H.H., Cath, T.Y. and Nghiem, L.D. (2014) A novel membrane distillation–thermophilic bioreactor system: Biological stability and trace organic compound removal. Bioresource Technology 159, 334-341.
Wu, B., Kitade, T., Chong, T.H., Uemura, T. and Fane, A.G. (2013) Impact of membrane bioreactor operating conditions on fouling behavior of reverse osmosis membranes in MBR–RO processes. Desalination 311, 37-45.
Wu, B., Suwarno, S.R., Tan, H.S., Kim, L.H., Hochstrasser, F., Chong, T.H., Burkhardt, M., Pronk, W. and Fane, A.G. (2017) Gravity-driven microfiltration pretreatment for reverse osmosis (RO) seawater desalination: Microbial community characterization and RO performance. Desalination 418, 1-8.
Wu, B., Yi, S. and Fane, A.G. (2011) Microbial behaviors involved in cake fouling in membrane bioreactors under different solids retention times. Bioresource Technology 102(3), 2511-2516.
Xia, S., Jia, R., Feng, F., Xie, K., Li, H., Jing, D. and Xu, X. (2012) Effect of solids retention time on antibiotics removal performance and microbial communities in an A/O-MBR process. Bioresource Technology 106, 36-43.
Xiao, K., Liang, S., Wang, X., Chen, C. and Huang, X. (2019) Current state and challenges of full-scale membrane bioreactor applications: A critical review. Bioresource Technology 271, 473-481.
Yu, X.-C. and Margolin, W. (1997) Ca2+-mediated GTP-dependent dynamic assembly of bacterial cell division protein FtsZ into asters and polymer networks in vitro. The EMBO Journal 16(17), 5455-5463.
Zaviska, F., Drogui, P., Grasmick, A., Azais, A. and Héran, M. (2013) Nanofiltration membrane bioreactor for removing pharmaceutical compounds. Journal of Membrane Science 429, 121-129.
Zhang, H., Fan, X., Wang, B. and Song, L. (2016) Calcium ion on membrane fouling reduction and bioflocculation promotion in membrane bioreactor at high salt shock. Bioresource Technology 200, 535-540.

Zhang, J., Chua, H.C., Zhou, J. and Fane, A.G. (2006) Factors affecting the membrane performance in submerged membrane bioreactors. Journal of Membrane Science 284(1–2), 54-66.

Zhang, J., Zhou, J., Liu, Y. and Fane, A.G. (2010) A comparison of membrane fouling under constant and variable organic loadings in submerge membrane bioreactors. Water Research 44(18), 5407-5413.

Electronic Supplementary Material (for online publication only)

Click here to download Electronic Supplementary Material (for online publication only): Appendix.docx